

Theory of the Valence Band Structure of Germanium in an External Magnetic Field*

R. F. WALLIS AND H. J. BOWLDEN†
U. S. Naval Research Laboratory, Washington, D. C.

(Received October 30, 1959)

The energies of the magnetic sub-bands associated with the V_1 and V_2 valence bands in germanium have been calculated as a function of k_z , the propagation constant parallel to the external magnetic field. Warping of the V_1 and V_2 bands was neglected. Sub-bands belonging to the 1^+ and 2^+ ladders (light holes) have minima at $k_z=0$ and show quantum effects consisting of a decrease in curvature as the valence band edge is approached. Sub-bands belonging to the 2^- ladder (heavy holes) also have minima at $k_z=0$, but the curvatures increase near the valence band edge. The 1^- heavy hole sub-bands show very marked quantum effects. The sub-band minima occur at values of k_z different from zero, and local maxima appear at $k_z=0$. The peculiar nature of the 1^- magnetic sub-bands may lead to observable effects in various magneto-optic phenomena in germanium.

I. INTRODUCTION

IN the presence of an external magnetic field the energies of electrons or holes in semiconductors are quantized into magnetic sub-bands or Landau levels. During the last few years a great deal of valuable information concerning semiconductors has been obtained through the study of optical transitions between magnetic sub-bands. For example, cyclotron resonance¹ involves optical transitions between sub-bands in the same band, while the interband magneto-optic effect² involves optical transitions between sub-bands in different bands. Also potentially useful is the study³ of optical transitions between bound impurity levels and the sub-bands of the valence or conduction bands.

In each of these phenomena the most intense absorption corresponds to transitions from or to the extrema of the sub-bands involved. This is a consequence of the fact that the magnetic sub-bands are essentially one-dimensional and have infinite densities of states at their extrema. Furthermore, the peak intensities are in part determined by the curvatures of the sub-bands at their extrema. It is therefore clear that in order to understand the positions and intensities of absorption in the various magneto-optic phenomena, one should have a detailed knowledge of the structure of the magnetic sub-bands.

In the present paper the structure of the magnetic sub-bands in the valence band of germanium is de-

veloped using the theory of Luttinger.⁴ It is found that the degeneracy of the valence band leads to some rather surprising "quantum" effects.

II. DERIVATION OF THE SECULAR EQUATION

According to Luttinger the effective mass Hamiltonian D for holes in the V_1 and V_2 valence bands in the presence of a constant external magnetic field \mathbf{H} can be written as

$$D = (1/m) [(\gamma_1 + \frac{5}{2}\gamma_2)(P^2/2) - \gamma_2(P_x^2J_x^2 + P_y^2J_y^2 + P_z^2J_z^2) - 2\gamma_3(\{P_xP_y\}\{J_xJ_y\} + \{P_yP_z\}\{J_yJ_z\} + \{P_zP_x\}\{J_zJ_x\}) + (e/c)\kappa\mathbf{J}\cdot\mathbf{H} + (eq/c) \times (J_x^3H_x + J_y^3H_y + J_z^3H_z)], \quad (1)$$

where $\gamma_1, \gamma_2, \gamma_3, \kappa$ and q are the effective mass parameters and J_x, J_y , and J_z are 4×4 matrices satisfying the commutation rules for angular momentum. The quantities P_x, P_y , and P_z are the components of the kinetic momentum operator $\mathbf{p} + (e/c)\mathbf{A}$ where \mathbf{A} is the vector potential of the external magnetic field. The symbol $\{P_xP_y\}$ represents the symmetrized product $\frac{1}{2}(P_xP_y + P_yP_x)$.

For germanium it is a reasonably good approximation⁴ to take $\gamma_2 = \gamma_3 = \bar{\gamma}$ and to take $q = 0$. We adopt the representation discussed by Luttinger in which

$$J_z = \begin{vmatrix} \frac{3}{2} & 0 & 0 & 0 \\ 0 & -\frac{1}{2} & 0 & 0 \\ 0 & 0 & \frac{1}{2} & 0 \\ 0 & 0 & 0 & -\frac{3}{2} \end{vmatrix}. \quad (2)$$

Under these conditions the Hamiltonian D can be rewritten in the form

$$D = D_0 + D_1 + D_2, \quad (3)$$

⁴ J. M. Luttinger, Phys. Rev. **102**, 1030 (1956).

* A preliminary account of this work was given at the March, 1959, meeting of the American Physical Society in Cambridge, Massachusetts. See Bull. Am. Phys. Soc. **4**, 145 (1959).

† Permanent address: National Carbon Research Laboratories, National Carbon Company, Division of Union Carbide Corporation, Parma, Ohio.

¹ See, for example, R. N. Dexter, H. J. Zeiger, and B. Lax, Phys. Rev. **95**, 557 (1954); G. Dresselhaus, A. F. Kip, and C. Kittel, Phys. Rev. **98**, 368 (1955); E. Burstein, G. S. Picus, and H. A. Gebbie, Phys. Rev. **103**, 185 (1956).

² See, for example, S. Zwerdling, B. Lax, and L. M. Roth, Phys. Rev. **108**, 1402 (1957); E. Burstein, G. S. Picus, R. F. Wallis, and F. Blatt, Phys. Rev. **113**, 15 (1959).

³ R. F. Wallis and H. J. Bowlden, J. Phys. Chem. Solids **7**, 78 (1958); W. S. Boyle, J. Phys. Chem. Solids **8**, 321 (1959); H. Y. Fan and P. Fisher, J. Phys. Chem. Solids **8**, 270 (1959).

where

$$D_0 = \frac{1}{2m} \begin{vmatrix} (\gamma_1 + \bar{\gamma})(P_x^2 + P_y^2) & -3\frac{1}{2}\bar{\gamma}(P_x - iP_y)^2 & 0 & 0 \\ +3\frac{1}{2}\hbar^2 s\kappa & (\gamma_1 - \bar{\gamma})(P_x^2 + P_y^2) & 0 & 0 \\ -3\frac{1}{2}\bar{\gamma}(P_x + iP_y)^2 & -\frac{1}{2}\hbar^2 s\kappa & (\gamma_1 - \bar{\gamma})(P_x^2 + P_y^2) & -3\frac{1}{2}\bar{\gamma}(P_x - iP_y)^2 \\ 0 & 0 & +\frac{1}{2}\hbar^2 s\kappa & 0 \\ 0 & 0 & -3\frac{1}{2}\bar{\gamma}(P_x + iP_y)^2 & (\gamma_1 + \bar{\gamma})(P_x^2 + P_y^2) \\ & & & -3\frac{1}{2}\hbar^2 s\kappa \end{vmatrix}, \quad (3a)$$

$$D_1 = \frac{1}{2m} \begin{vmatrix} (\gamma_1 - 2\bar{\gamma})P_z^2 & 0 & 0 & 0 \\ 0 & (\gamma_1 + 2\bar{\gamma})P_z^2 & 0 & 0 \\ 0 & 0 & (\gamma_1 + 2\bar{\gamma})P_z^2 & 0 \\ 0 & 0 & 0 & (\gamma_1 - 2\bar{\gamma})P_z^2 \end{vmatrix}, \quad (3b)$$

$$D_2 = \frac{1}{2m} \begin{vmatrix} 0 & 0 & -2\bar{\gamma}3\frac{1}{2}(P_x - iP_y)P_z & 0 \\ 0 & 0 & 0 & 2\bar{\gamma}3\frac{1}{2}(P_x - iP_y)P_z \\ -2\bar{\gamma}3\frac{1}{2}(P_x + iP_y)P_z & 0 & 0 & 0 \\ 0 & 2\bar{\gamma}3\frac{1}{2}(P_x + iP_y)P_z & 0 & 0 \end{vmatrix}, \quad (3c)$$

and $s = eH/\hbar c$.

We shall assume a constant external magnetic field in the z direction and shall choose the gauge $\mathbf{A} = (-Hy, 0, 0)$. The eigenvectors of D are then conveniently expressed in terms of the functions

$$G_l = \frac{\exp[i(k_x x + k_z z)]}{(L_x L_z)^{\frac{1}{2}}} \left(\frac{s^{\frac{1}{2}}}{2^l l! \pi^{\frac{1}{2}}} \right)^{\frac{1}{2}} H_l(t) \exp(-t^2/2), \quad (4)$$

where $t = s^{\frac{1}{2}}y - (k_x/s^{\frac{1}{2}})$ and $H_l(t)$ is the Hermite polynomial of degree l . The functions G_l satisfy the following relations:

$$(P_x^2 + P_y^2)G_l = \hbar^2 s(2l+1)G_l, \quad (5)$$

$$(P_x + iP_y)G_l = -\hbar s^{\frac{1}{2}}[2(l+1)]^{\frac{1}{2}}G_{l+1}, \quad (6)$$

$$(P_x - iP_y)G_l = -\hbar s^{\frac{1}{2}}(2l)^{\frac{1}{2}}G_{l-1}, \quad (7)$$

$$P_z G_l = \hbar s^{\frac{1}{2}} \zeta G_l, \quad (8)$$

where $\zeta = k_z/s^{\frac{1}{2}}$.

As indicated by Luttinger the eigenvectors of D as given in Eqs. (3) can be written in the form

$$\psi = \begin{vmatrix} c_1 G_{l-2} \\ c_2 G_l \\ c_3 G_{l-1} \\ c_4 G_{l+1} \end{vmatrix}, \quad (9)$$

where the c_i are numerical coefficients. If one substitutes Eq. (9) into the Schrödinger equation

$$D\psi = \epsilon\psi, \quad (10)$$

and makes use of Eqs. (5)–(8), one finds that the eigenvalues of D are determined by solution of the secular equation

$$\begin{vmatrix} (\gamma_1 + \bar{\gamma})(l - 2 + \frac{1}{2}) & -\bar{\gamma}[3l(l-1)]^{\frac{1}{2}} & \bar{\gamma}[6(l-1)]^{\frac{1}{2}}\zeta & 0 \\ +\frac{1}{2}(\gamma_1 - 2\bar{\gamma})\zeta^2 + \frac{3}{2}\kappa - \epsilon & & & \\ -\bar{\gamma}[3l(l-1)]^{\frac{1}{2}} & (\gamma_1 - \bar{\gamma})(l + \frac{1}{2}) & 0 & -\bar{\gamma}[6(l+1)]^{\frac{1}{2}}\zeta \\ +\frac{1}{2}(\gamma_1 + 2\bar{\gamma})\zeta^2 - \frac{1}{2}\kappa - \epsilon & & & \\ \bar{\gamma}[6(l-1)]^{\frac{1}{2}}\zeta & 0 & (\gamma_1 - \bar{\gamma})(l - 1 + \frac{1}{2}) & -\bar{\gamma}[3l(l+1)]^{\frac{1}{2}} \\ +\frac{1}{2}(\gamma_1 + 2\bar{\gamma})\zeta^2 + \frac{1}{2}\kappa - \epsilon & & & \\ 0 & -\bar{\gamma}[6(l+1)]^{\frac{1}{2}}\zeta & -\bar{\gamma}[3l(l+1)]^{\frac{1}{2}} & (\gamma_1 + \bar{\gamma})(l + 1 + \frac{1}{2}) \\ & & & +\frac{1}{2}(\gamma_1 - 2\bar{\gamma})\zeta^2 - \frac{3}{2}\kappa - \epsilon \end{vmatrix} = 0, \quad (11)$$

where the energy ϵ is measured in units of $\hbar eH/mc$. The quantity l corresponds to the Landau magnetic quantum number. For $l=-1$ there is one physically meaningful solution to Eq. (11), for $l=0$ there are two solutions, for $l=1$ there are three solutions and for $l=2, 3, 4, \dots$ there are four solutions.

$$\left| \begin{array}{c} (\gamma_1 + \bar{\gamma})(l - 2 + \frac{1}{2}) + \frac{1}{2}(\gamma_1 - 2\bar{\gamma})\zeta^2 + \frac{3}{2}\kappa - \epsilon \\ -\bar{\gamma}[3l(l-1)]^{\frac{1}{2}} \end{array} \right| = 0, \quad (12)$$

and

$$\left| \begin{array}{c} (\gamma_1 - \bar{\gamma})(l - 1 + \frac{1}{2}) + \frac{1}{2}(\gamma_1 + 2\bar{\gamma})\zeta^2 + \frac{1}{2}\kappa - \epsilon \\ -\bar{\gamma}[3l(l+1)]^{\frac{1}{2}} \end{array} \right| = 0. \quad (13)$$

The solutions of Eq. (12) may be designated by $\epsilon_1^+(l)$ and $\epsilon_1^-(l)$ in accordance with Luttinger while the solutions of Eq. (13) may be designated by $\epsilon_2^+(l)$ and $\epsilon_2^-(l)$. It is convenient in calculating $\epsilon_2^+(l)$ and $\epsilon_2^-(l)$ from Eq. (11) or Eq. (13) to replace l by $l-1$. If this is done, physically meaningful values of both $\epsilon_1^+(l)$ and $\epsilon_2^+(l)$ correspond to $l=0, 1, 2, 3, \dots$ while meaningful values of both $\epsilon_1^-(l)$ and $\epsilon_2^-(l)$ correspond to $l=2, 3, 4, \dots$. This notation for the magnetic levels now agrees with that of Luttinger (except for replacing n by l) and will be followed in the remainder of the paper. A diagram of the energy levels obtained by solving Eqs. (12) and (13) is given in Fig. 1 for germanium. The effective mass parameters were assigned the values $\gamma_1=13.20$, $\bar{\gamma}=4.92$, $\kappa=3.30$ which were calculated from data kindly supplied by Dr. Evan O. Kane. The plus levels form two light

hole "ladders" with a relatively large spacing between adjacent levels while the minus levels form two heavy hole "ladders" with a relatively small spacing between adjacent levels. The quantum effects discussed by Luttinger are manifested by the nonuniform spacing of levels in a given ladder.

If ζ is not zero, it is more difficult to obtain exact analytic solutions to Eq. (11). Since exact solutions are available for $\zeta=0$, however, one can use perturbation theory to obtain the energy levels correct to second order in ζ . Such solutions are satisfactory for small ζ . Alternatively, one can solve Eq. (11) numerically and obtain results valid for a larger range of ζ . We have carried out treatments of both types.

III. PERTURBATION THEORY FOR SMALL ζ

The eigenvalues of the zero order Hamiltonian D_0 are determined by the solutions of Eqs. (12) and (13). The corresponding zero order eigenfunctions can be written as

III. PERTURBATION THEORY FOR SMALL ζ

The eigenvalues of the zero order Hamiltonian D_0 are determined by the solutions of Eqs. (12) and (13). The corresponding zero order eigenfunctions can be written as

$$\psi_1^\pm = \begin{pmatrix} c_1^\pm G_{l-2} \\ c_2^\pm G_l \\ 0 \\ 0 \end{pmatrix}, \quad (14a)$$

$$\psi_2^\pm = \begin{pmatrix} 0 \\ 0 \\ c_3^\pm G_{l-2} \\ c_4^\pm G_l \end{pmatrix}. \quad (14b)$$

The operators D_1 and D_2 may be treated as perturbations, and correction terms calculated by standard matrix perturbation theory. It may be noted that the diagonal matrix elements of D_1 with respect to the eigenfunctions of D_0 lead to first order corrections to the energy which are proportional to ζ^2 . The diagonal matrix elements of D_2 vanish so that the first order energy corrections from D_2 are zero. Nonvanishing matrix elements of D_2 exist between the following pairs of states: $1^+(l), 2^+(l+1)$; $1^+(l), 2^-(l+1)$; $1^-(l), 2^+(l+1)$; $1^-(l), 2^-(l+1)$. Second order energy corrections from D_2 are proportional to ζ^2 .

The results of the second order perturbation treat-

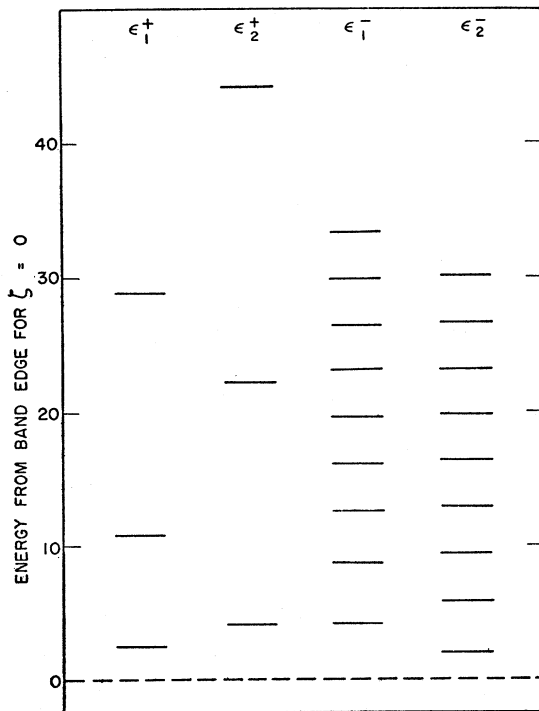


FIG. 1. Energies of the magnetic sub-bands for the valence band in germanium measured from the band edge in units of $\hbar eH/mc$.

ment of D_1 and D_2 can be expressed as

$$\epsilon(l, \zeta) = \epsilon(l) + (\hbar^2 s / 2m^*) \zeta^2, \quad (15)$$

where $\epsilon(l)$ stands for $\epsilon_1^\pm(l)$ or $\epsilon_2^\pm(l)$ as appropriate and m^* is the curvature effective mass of the magnetic sub-band at $\zeta=0$. In Table I the values of m^*/m are given for magnetic sub-bands in germanium which lie near the valence band edge. One sees that the light hole sub-bands (+ levels) near the band edge show quantum effects in their curvature effective mass ratios, but far from the edge the effective mass ratios approach the value 0.04 given by cyclotron resonance measurements.¹ The increase in effective mass near the band edge is consistent with the decrease in separation between light hole sub-bands at $\zeta=0$ as shown in Fig. 1. The largest quantum effect is shown by the $2^+(0)$ level which has a curvature characteristic of a heavy hole rather than a light hole.

The results for the heavy hole sub-bands (- levels) are quite surprising. The effective mass ratios are much smaller in magnitude than the value 0.3 given by cyclotron resonance¹ and show no tendency to approach this value away from the band edge. For the 1^- levels the effective masses are negative indicating that these sub-bands have a curvature at $\zeta=0$ opposite to that normally expected for holes.

The reason for the anomalous behavior of the heavy hole sub-bands can be seen by inspection of Fig. 1. One notes that pairs of heavy hole levels [the $1^-(l)$ and the $2^-(l+1)$ levels, $l=2, 3, 4, \dots$] are very nearly degenerate and that the tendency toward degeneracy increases away from the band edge. Furthermore, these pairs of nearly degenerate levels are coupled by the perturbation D_2 so that the second order corrections to the energy involve energy differences in the denominators which nearly vanish. For small ζ , these interactions between pairs of nearly degenerate levels give the dominant second order corrections to the energies. Consequently, in one ladder of levels the energies increase rapidly as $|\zeta|$ increases from zero while in the other ladder the energies decrease rapidly.

IV. EXACT SOLUTIONS

The strong interaction between the pairs of levels $1^-(l)$ and $2^-(l+1)$ leads to a breakdown of second order perturbation theory for only moderate values of $|\zeta|$. In order to extend the calculations to larger values of $|\zeta|$, exact solutions to Eq. (11) were obtained numerically

TABLE I. Curvature effective mass ratios m^*/m at $\zeta=0$.

l	1^+	2^+	1^-	2^-
0	0.120	0.298		
1	0.076	0.055		
2	0.045	0.048	-0.064	0.065
3	0.043	0.046	-0.038	0.041
4	0.043	0.045	-0.027	0.030
5			-0.021	0.023

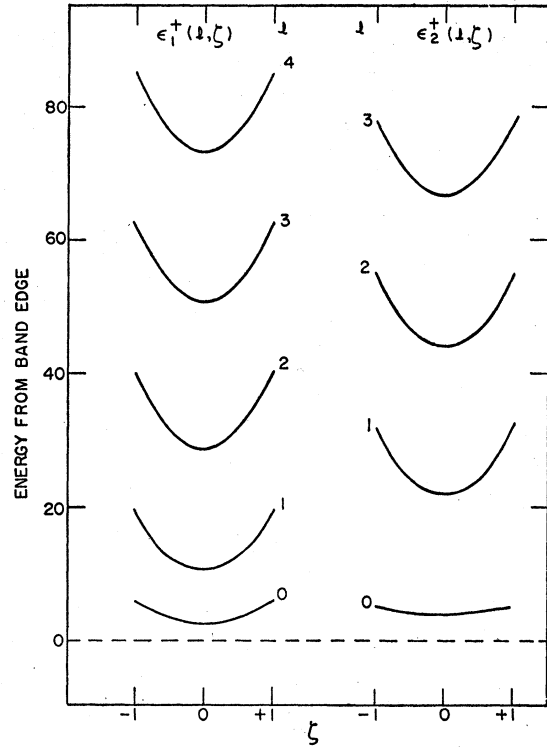


FIG. 2. Energies of the light hole magnetic sub-bands as functions of ζ . The energies are measured from the band edge in units of $\hbar eH/mc$.

using the NAREC digital computer at the Naval Research Laboratory. We are indebted to Dr. Benjamin Lepson who provided us with the numerical solutions.

The results of the numerical calculations for the light hole magnetic sub-bands are shown in Fig. 2. These sub-bands are nearly parabolic with curvatures corresponding to the effective masses listed in Table I. The quantum effects in the curvature effective masses and in the energy separations at $\zeta=0$ are the principal differences from the magnetic sub-bands for non-degenerate parabolic bands.

The results for the heavy hole magnetic sub-bands are shown in Fig. 3. The 2^- levels approximate parabolas in a very rough manner. The curvature of a given level is not constant but decreases rapidly as $|\zeta|$ increases from zero. The 1^- levels are characterized by local maxima at $\zeta=0$ and local minima at symmetrically located values of ζ away from $\zeta=0$. For sub-bands near the band edge, the energy separation between the maximum and minimum of a given sub-band is about 20% of the separation of adjacent sub-bands at $\zeta=0$. The curvature varies not only in magnitude but also in sign. For $|\zeta| \gg 1$, the curvature is approximately that corresponding to the classical heavy hole mass value of $0.3m$.

The curvature effective masses at the local minima away from $\zeta=0$ are of special interest and are tabulated in Table II together with the positions of the minima.

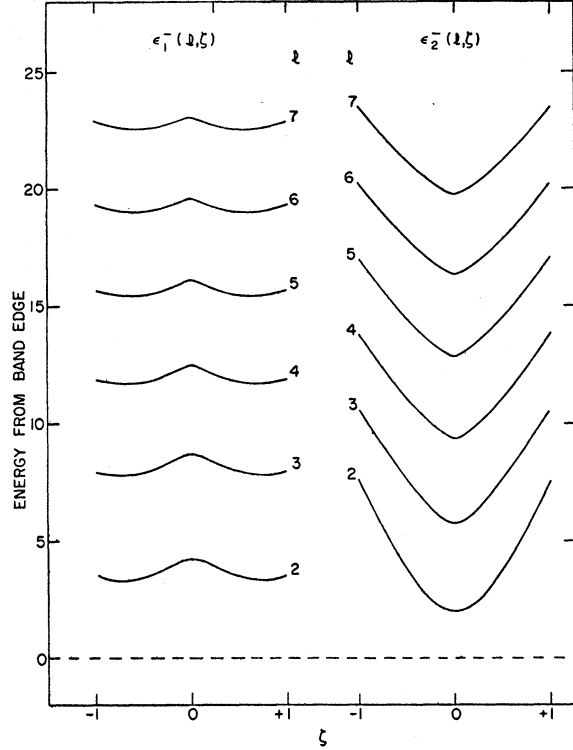


FIG. 3. Energies of the heavy hole magnetic sub-bands as functions of ζ . The energies are measured from the band edge in units of $\hbar eH/mc$.

The effective mass ratios increase away from the band edge and approach the classical value 0.3. The range of ζ values for which the curvatures are anomalous decreases the farther the sub-band lies from the band edge. The anomalous effects in the 1^- sub-bands therefore vanish in the limit of large l values. This is in accordance with the quantum nature of these effects.

The exact results for the energies of the heavy hole sub-bands can be presented in an approximate analytic form if one carries out an exact diagonalization of the Hamiltonian D with respect to the states $1^-(l)$ and $2^-(l+1)$ and treats the remaining interactions by second order perturbation theory. The energies can then be written in the approximate forms

$$\epsilon_1^-(l, \zeta) \simeq A_1 + B_1 \zeta^2 - \frac{1}{2}(R + S \zeta^2)^{\frac{1}{2}}, \quad (16a)$$

$$\epsilon_2^-(l+1, \zeta) \simeq A_2 + B_2 \zeta^2 + \frac{1}{2}(R + S \zeta^2)^{\frac{1}{2}}, \quad (16b)$$

where the quantities A_1 , A_2 , B_1 , B_2 , R_1 , R_2 , S_1 , S_2 are rather complicated functions of the effective mass parameters and the magnetic quantum number l . For very small ζ , the square roots in Eqs. (16) can be expanded in powers of ζ^2 yielding results equivalent to those given by second order perturbation theory. For larger ζ , the square root terms become proportional to $|\zeta|$ and are then insignificant compared to $B_1 \zeta^2$ and $B_2 \zeta^2$ if ζ is sufficiently large.

It is instructive to consider the forms of Eqs. (16) if l is large, i.e., the magnetic sub-bands are far from the band edge. The following relations are then approximately valid:

$$A_1 = A_2 \simeq (\gamma_1 - 2\bar{\gamma})l, \quad (17a)$$

$$B_1 = B_2 \simeq \frac{1}{2}(\gamma_1 - 2\bar{\gamma}), \quad (17b)$$

$$R \simeq \frac{(2\bar{\gamma} + \gamma_1 - \kappa)^6}{(32\bar{\gamma}^2)^2} \frac{1}{l^4}, \quad (17c)$$

$$S \simeq \frac{9(\gamma_1 - \kappa)^2}{2l}. \quad (17d)$$

One sees that for sufficiently large l , the terms involving the square roots in Eqs. (16) become negligibly small compared to the other terms. The sub-band energies can then be written in the form

$$\epsilon_1^-(l) = \epsilon_2^-(l+1) \simeq (\gamma_1 - 2\bar{\gamma})l + \frac{1}{2}(\gamma_1 - 2\bar{\gamma})\zeta^2, \quad (18)$$

corresponding to simple parabolic magnetic sub-bands with a mass ratio $(m^*/m) = (\gamma_1 - 2\bar{\gamma})^{-1} = 0.298$. We thus have a confirmation of the statement that the quantum effects vanish far from the band edge.

V. DISCUSSION

The quantum effects investigated in this paper may lead to observable phenomena in magneto-optic studies of germanium and similar semiconductors. This is particularly true of optical transitions from or to the 1^- magnetic sub-bands. These sub-bands have infinite densities of states at the local maxima at $\zeta=0$ and at the minima away from $\zeta=0$. It has been recognized previously² that the infinite effective densities of states for vertical transitions at $\zeta=0$ lead to sharply peaked absorption lines in the interband magneto-optic (IMO) effect corresponding to transitions from the 1^- levels in the valence band to the magnetic sub-bands associated with the conduction band minimum at $k=0$. From the present work it may be seen that the shapes of the 1^- sub-bands are such that the effective density of states for optical transitions to other magnetic sub-bands may be infinite for vertical transitions at certain ζ values not equal to zero. These infinite effective densities of states for optical transitions away from $\zeta=0$ may be expected to lead to new absorption peaks in the IMO effect.

TABLE II. Curvature effective mass ratios m^*/m for heavy hole minima not at $\zeta=0$.

l	m^*/m	ζ_{\min}
2	0.198	0.74
3	0.223	0.74
4	0.245	0.70
5	0.259	0.65
6	0.269	0.61
7	0.276	0.57

Similar phenomena should occur in the cyclotron resonance of holes in germanium. In his discussion of the quantum theory of cyclotron resonance Goodman⁵ has recognized that the absorption line shapes may be modified by $\zeta \neq 0$ effects. New absorption lines may arise due to transitions involving the 1^- levels and having infinite effective densities of states for $\zeta \neq 0$.

New peaks may also be expected in the photoionization absorption spectrum of acceptor impurities in germanium in an external magnetic field.⁶ Investigations are currently underway on the various topics just discussed.

The calculations presented in this paper have been based on the assumption that $\gamma_2 = \gamma_3$. This is equivalent to neglecting the warping of the valence band. The question arises whether lifting the restriction $\gamma_2 = \gamma_3$ has any important effect on the results presented. A partial answer may be obtained by considering the effect of $\gamma_2 \neq \gamma_3$ on the sub-band energies at $\zeta = 0$. Goodman⁷ has made calculations of these energies with γ_2 and γ_3 chosen to fit the cyclotron resonance data of Fletcher, Yager, and Merritt⁸ and with the magnetic field in the (100), (110), and (111) directions. For the (100) and (110) directions the sub-band energies are shifted only slightly compared to the case in which γ_2 and γ_3 are replaced by $\frac{1}{2}(\gamma_2 + \gamma_3)$. In particular, the energies $\epsilon_1^-(l)$ and $\epsilon_2^-(l+1)$ are again very nearly equal. Since these levels are still coupled by the ζ perturbation, one should

again find large quantum effects in the dependence of the heavy hole sub-bands on ζ . For the (111) direction the energies are shifted somewhat more than in the (100) and (110) directions, but the near degeneracy of the $1^-(l)$ and $2^-(l+1)$ levels is not greatly affected. Large quantum effects in the heavy hole sub-bands may therefore be expected in the (111) direction also.

A comment may be made concerning the relationship between the negative mass holes of the 1^- sub-bands near $\zeta = 0$ and the negative mass holes studied by Dousmanis et al.⁹ through cyclotron resonance. In the latter case the negative mass holes are a consequence of the warping of the valence band. The negative masses for holes discussed in the present paper do not arise from the warping of the valence band and apply only to motion of the holes parallel to the magnetic field. It, therefore, appears that the two types of negative effective masses are different manifestations of the complexity of the valence band in germanium.

VI. ACKNOWLEDGMENTS

It is a pleasure to thank Elias Burstein who initiated the magneto-optic studies of semiconductors at the Naval Research Laboratory and whose stimulating comments contributed much to this work. We also thank R. R. Goodman, E. O. Kane, W. Kohn, J. M. Luttinger, and G. S. Picus for helpful discussions. We are indebted to Dr. Benjamin Lepson through whom the calculations on the NAREC digital computer were carried out and to M. C. Wallis for help with the perturbation theory calculations.

⁵ R. R. Goodman, Ph.D. dissertation, University of Michigan, Ann Arbor, Michigan, 1958 (unpublished).

⁶ R. F. Wallis and H. J. Bowlden, *J. Phys. Chem. Solids* **8**, 318 (1959).

⁷ R. R. Goodman (private communication).

⁸ R. C. Fletcher, W. A. Yager, and F. R. Merritt, *Phys. Rev.* **100**, 747 (1955).

⁹ G. C. Dousmanis, R. C. Duncan, J. J. Thomas, and R. C. Williams, *Phys. Rev. Letters* **1**, 404 (1958).